Decorating Self-Assembled Peptide Cages with Proteins

*James F. Ross,[1] Angela Bridges,[2] Jordan M. Fletcher,[1] Deborah Shoemark,[3,4] Dominic Alibhai,[5] Harriet E. V. Bray,[1] Joseph L. Beesley,[1] William M. Dawson,[1] Lorna R. Hodgson,[4] Judith Mantell,[5] Paul Verkade,[5] Colin M. Edge,[2] Richard B. Sessions,[3,4] David Tew[2] and Derek N. Woolfson[1,3,4]**

[1]School of Chemistry, University of Bristol, Cantock's Close, Bristol BS8 1TS, UK

[2] GSK, Gunnels Wood Rd, Stevenage, SG21 2NY, UK

[3]BrisSynBio, Life Sciences Building, Tyndall Avenue, Bristol BS8 1TQ, UK

[4]School of Biochemistry, University of Bristol, Biomedical Sciences Building, University Walk, Bristol, BS8 1TD, UK

[5]Wolfson Bioimaging Facility, University of Bristol, Biomedical Sciences Building, University Walk, Bristol, BS8 1TD, UK

*Address correspondence to d.n.woolfson@bristol.ac.uk or david.tew@gsk.com

Keywords: coiled coil; nanoreactor; protein cage; protein design; self-assembly; supramolecular assembly; synthetic biology.

Name	M	1	2
GFP-CC-Tri	-	GFP	-
CC-Tri-GFP	-	-	GFP
GFP-control	-	-	GFP
MBP-mCh-CC-Tri	MBP	mCherry	-
MBP-Luc-CC-Tri	MBP	Luciferase	-
MBP-CC-Tri-Luc	MBP	-	Luciferase

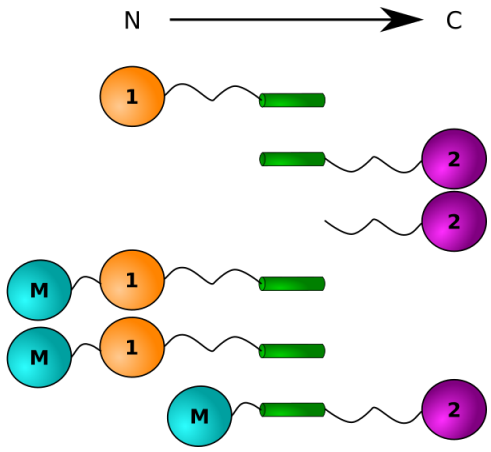

Figure S1: Schematics for fusion proteins used in this study. Nomenclature and schematics of fusion proteins depicting the orientation of the proteins used in this study relative the CC-Tri motif. A detailed description of the individual constructs can be found in Figures S13-20.

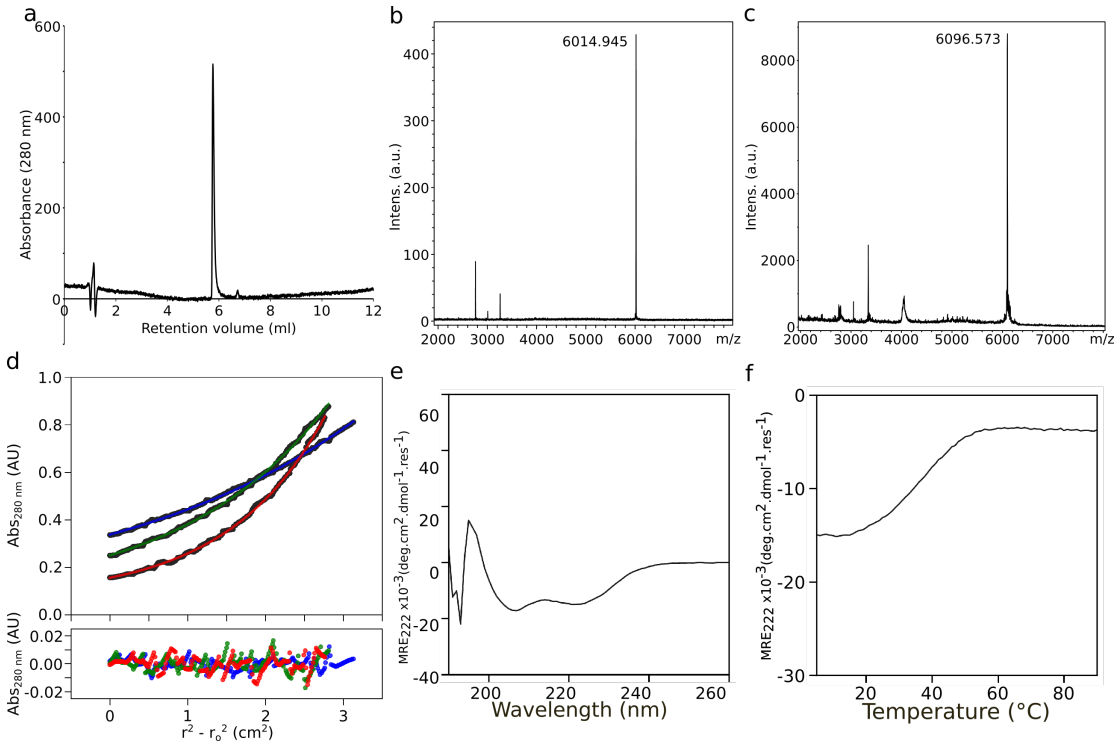

Figure S2: Characterisation of K4-HubB and HubB-TAMRA. (a) Analytical HPLC of K4-HubB showing a single peak. (**b)** MALDI-TOF mass spectrometry of K4-HubB, calculated mass 6012.38, observed mass 6014.95. **c)** MALDI-TOF mass spectrometry of HubB-TAMRA, calculated mass 6097.34, observed mass 6096.573. (**d)** Sedimentation equilibrium analytical ultracentrifugation (top, dots), fitted single-ideal species model curves at 26k (blue), 34k (green) and 42k (red) rpm. The fit returns a mass of 5821 Da (2.8 x monomer mass, 95% confidence limits 8908-9012). **(e)** CD spectrum of 50 μM K4-CC-Tri at 20°C. **(f)** Thermal melt of 50 μM K4-CC-Tri from 5°C to 90°C with a T_M of 36.5°C determined.

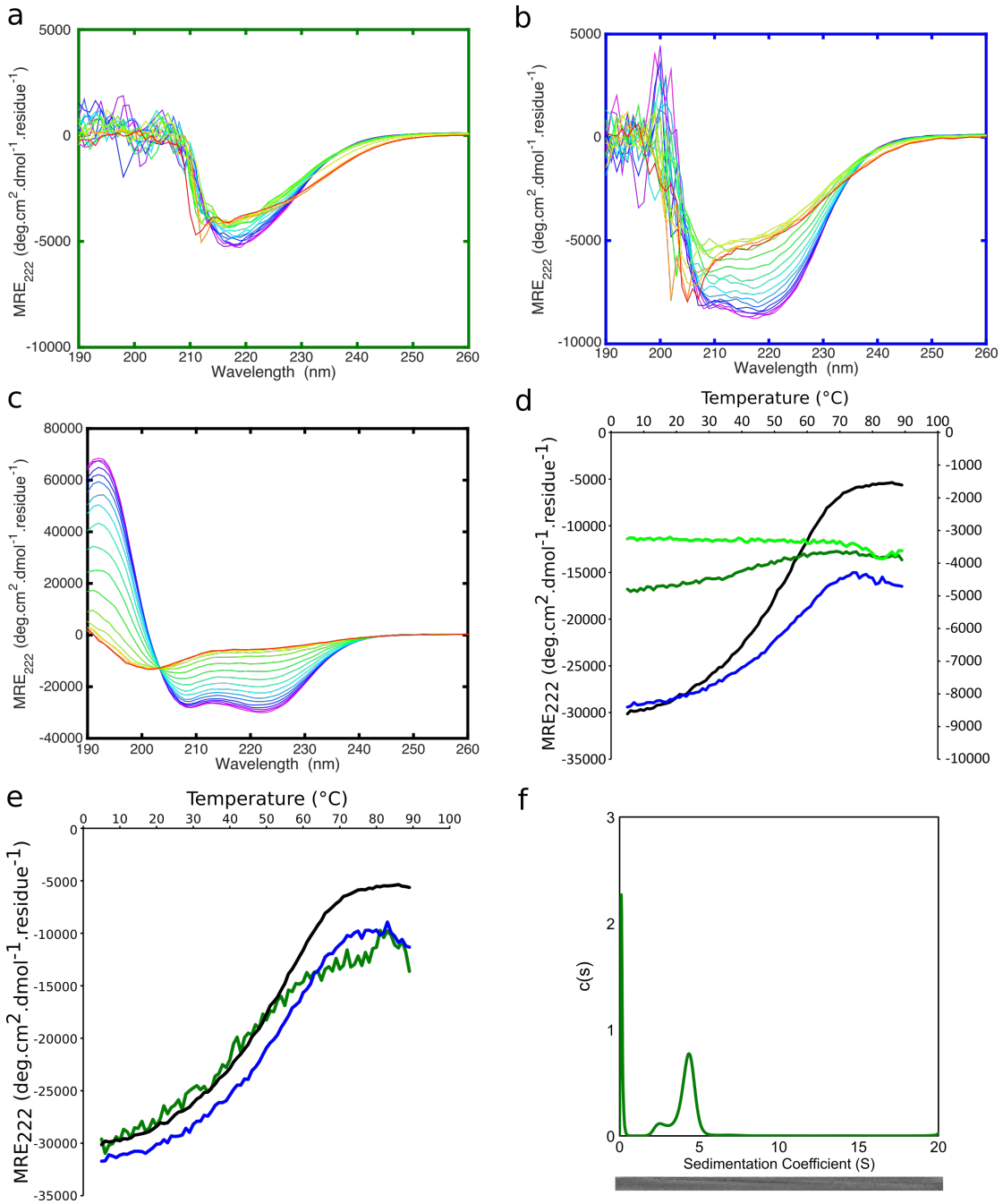

Figure S3: Thermal melts of individual and mixed CC-Tri components monitored by circular dichrosim, all experiments contain a final concentration of 50 µM of the CC-Tri motif in 25 mM HEPES, 100 mM NaCl (pH7.4). CD wavelength scan of a thermal melt in 5 °C intervals from 5°C (purple) to 90°C (red) for **(a)** GFP-CC-Tri **(b)** 1 : 2, GFP-CC-Tri : CC-Tri **(c)** CC-Tri. The colored frames relate to the respective curves on pannel e and f. (**d)** CD derived mean residue elipticity (MRE) at 222 nm for a thermal melt of, on the right-hand y-axis, GFP-control (bright green), CC-Tri-GFP (dark green), 1 : 2, GFP-CC-Tri : CC-Tri (blue) and, on the left-hand y-axis, CC-Tri (black). **(e)** CD derived MRE of GFP-CC-Tri (dark green) and 1 : 2, GFP-CC-Tri : CC-Tri (blue) normalised for the contribution of the CC-Tri motif only; overlayed with the CD derived MRE for CC-Tri. **(f)** Continuous c(s) distribution from sedimentation-velocity data at 35k rpm returning s = 4.27 S, $s_{20,w}$ = 5.58 S, f/f0 = 1.287 and mw = 85636 Da (2.46 × monomer mass) at 95% confidence level.

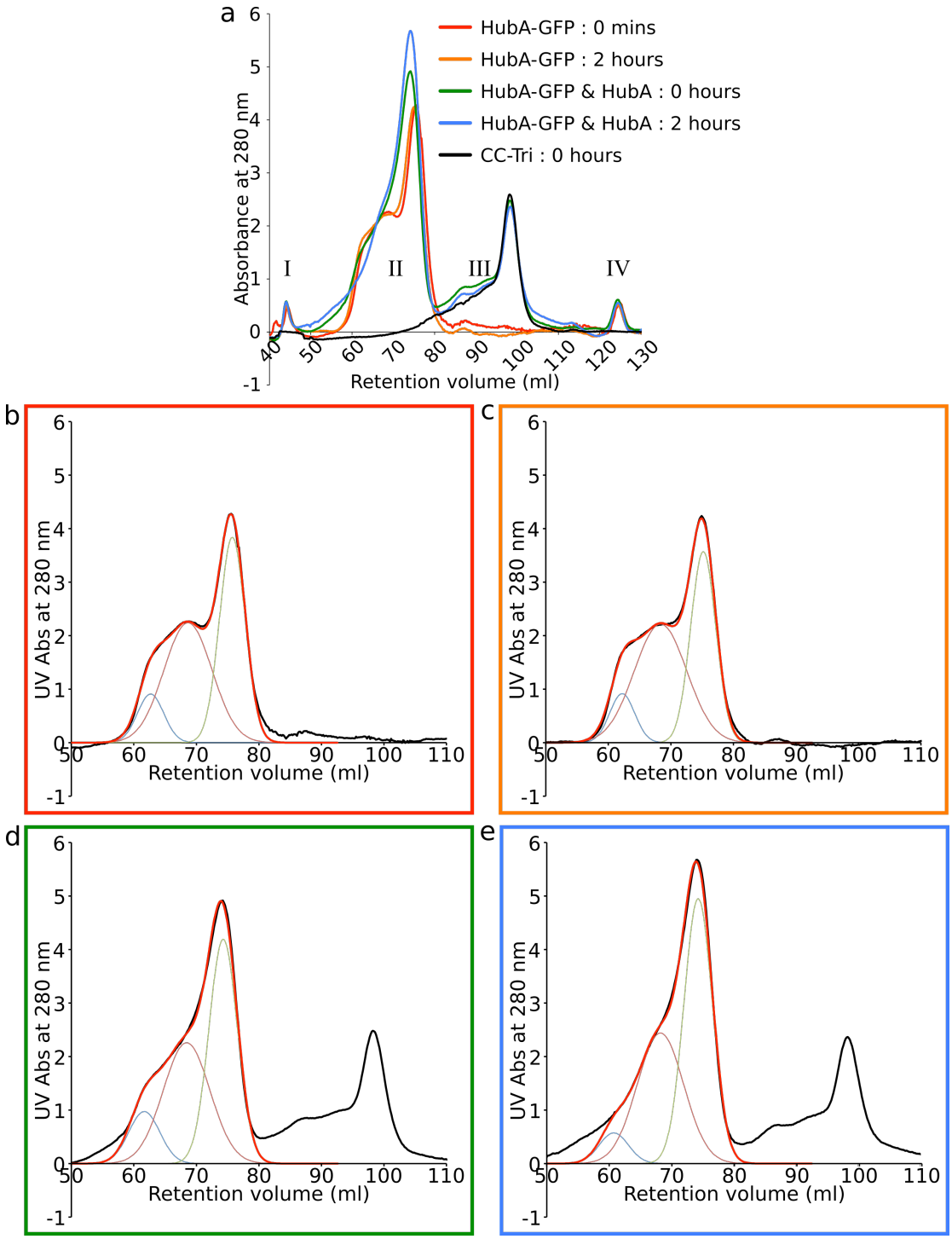

Figure S4: Size exclusion chromatography of individual and mixed CC-Tri components. **(a)** SEC of individual components, (black) 500 µl of 250 µM parent-HubA, (red) 500 µl of 25 µM HubA-GFP ran immediately upon dilution and (orange) after 2 hours incubation at 20 °C, (green) 500 µl containing 225 µM parent-HubA and 25 µM GFP-HubA ran immediately upon mixing and finally (blue) after 2 hours incubation at 20°C. **Key:** I, Void volume; II, HubA-GFP trimer/dimer/monomer; III, CC-Tri3; IV, contaminant. **(b)** HubA-GFP, **(c)** HubA-GFP 2 hour incubation, **(d)** HubA-GFP with HubA and **(e)** HubA-GFP with HubA 2 hour incubation. Raw trace (blank), individual gaussian fits for the trimer (blue), the dimer (burgandy) and the monomer (green), the sum of the Gaussian fits (red). The coloured frames relate to the respective curves on pannel (a).

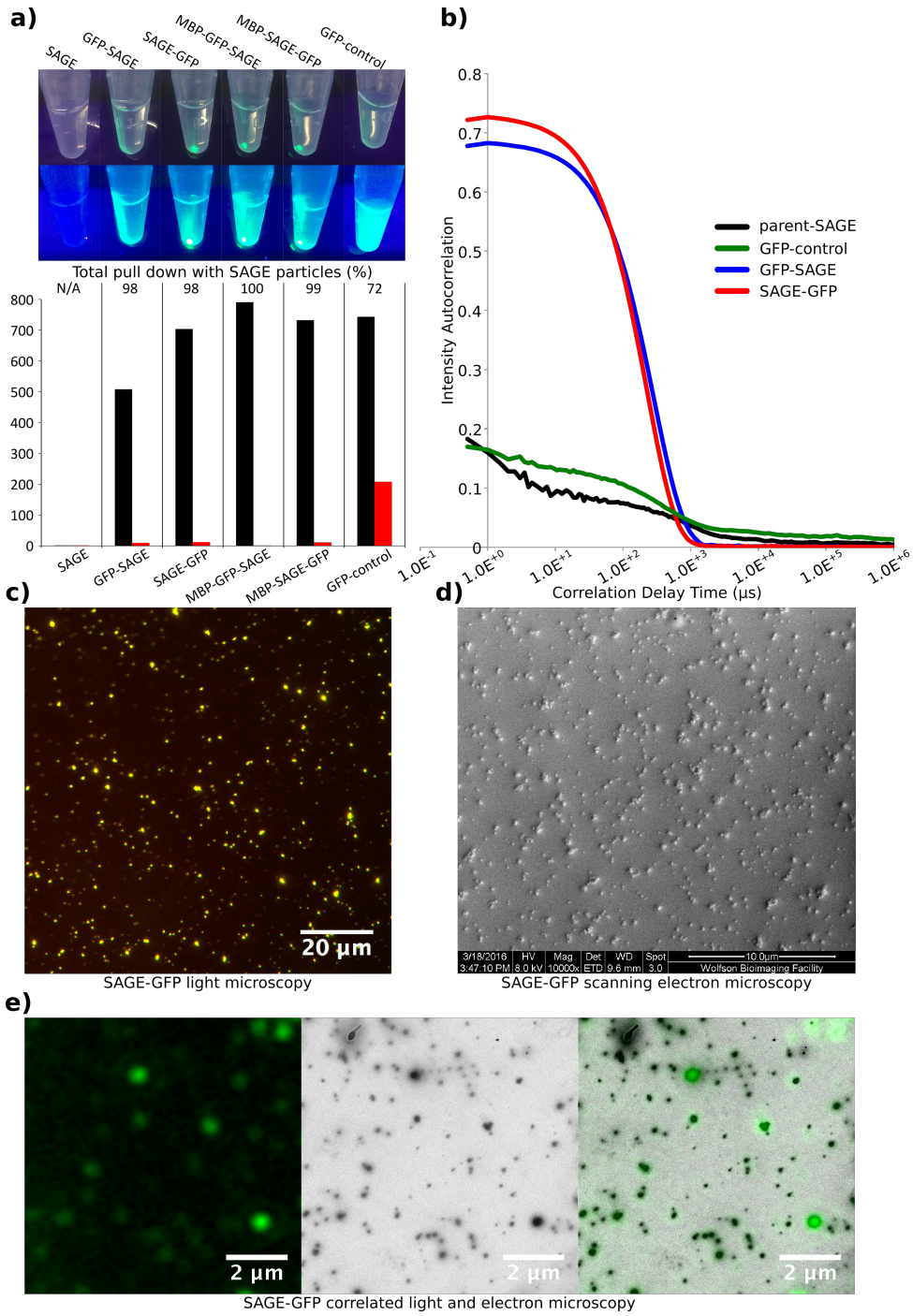

Figure S5: Additional characterisation of pSAGE particles. **a)** 200 µl of 25 µM 5% protein fusion SAGE particles were centrifuged for 6000 x g for 6 minutes. pSAGE particles produced fluorescent pellets (top) and measurements of the fluorescence remaining in the supernatant after centrifugation (bottom, red) compared to controls (bottom, black). **b)** Comparison between the autocorrelation function from DLS between the unsuitable data (parent-SAGE, black, and GFP-control, green) and the better quality data (GFP-SAGE, blue, and SAGE-GFP, red). Samples were prepared in 200 µl, at 3 µM SAGE concentration with 5% protein fusion. **c)** Low magnification example of duel colour fluorescence with 5% HubB-TAMRA (red) and 5% SAGE-GFP (green) particles, showing colocalisation between HubB and HubA-GFP. Samples were prepared at 25 µM SAGE. **d)** Low magnification example of fields of particles of 25 µM, 5% SAGE-GFP observed under SEM. **e)** Correlative light and electron microscopy (CLEM) of 25 µM, 5% SAGE-GFP particles first observed by light microscopy and later stained with 1% uranyl acetate, then visualized with TEM. LM and TEM images were then registered using FIJI.

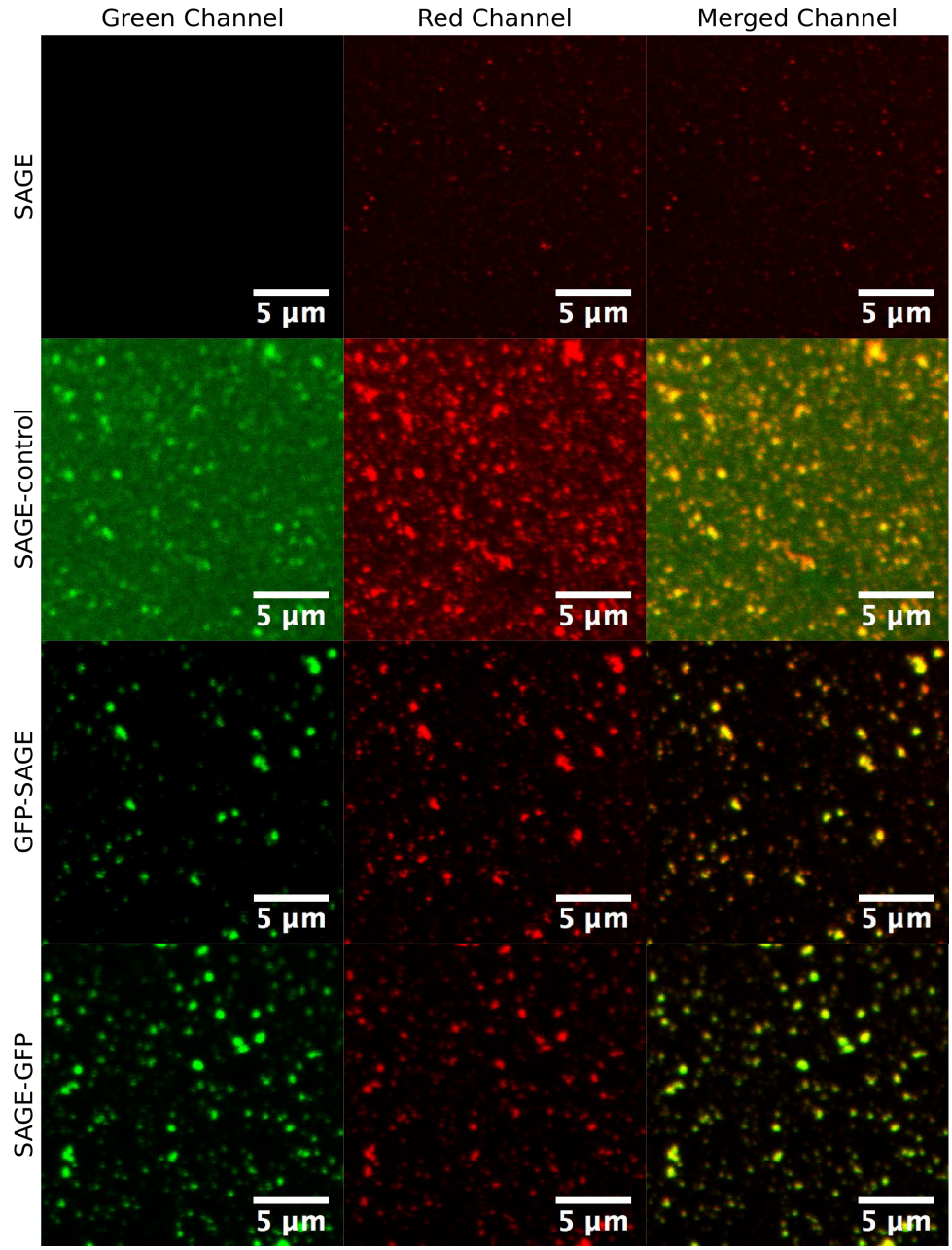

Figure S6: Dual color SAGE particles with TAMRA labelled K4-HubB and GFP labelled HubA. The green channel captures light between 492-550 nm when excited by a 488 nm laser. The red channel captures light between 565-650 nm when excited by a 561 nm laser. The merged channel overlays these two images. Of note is that all SAGE particles contain both TAMRA and GFP in the respective samples. In addition, in the GFP-control sample, there is evidance on non-associated GFP which provides a background of green light.

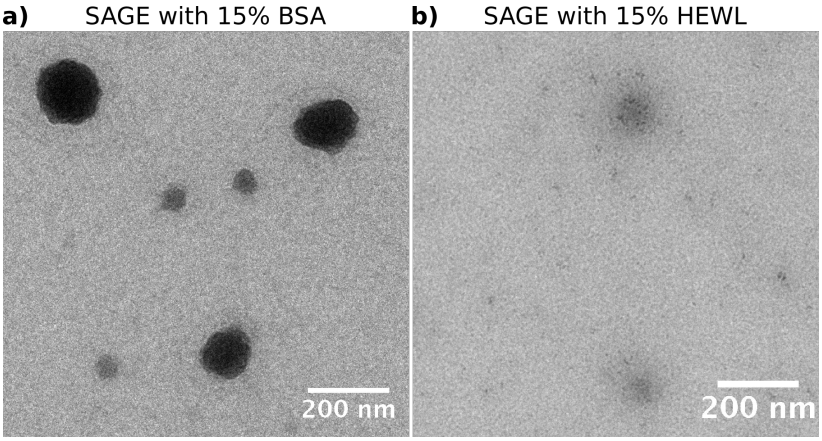

Figure S7: TEM of SAGE particles assembled in the presence of proteins with different isoelectric points. (a) 25 μM SAGE particles visualised by TEM when assembled in the presence of 1.25 μM bovine serum albumin (BSA, pI 4.7). **(b)** 25 μM SAGE particles, or lack thereof, visualised by TEM when assembled in the presence of 1.25 μM hen egg white lysozyme (HEWL, pI 11.35).

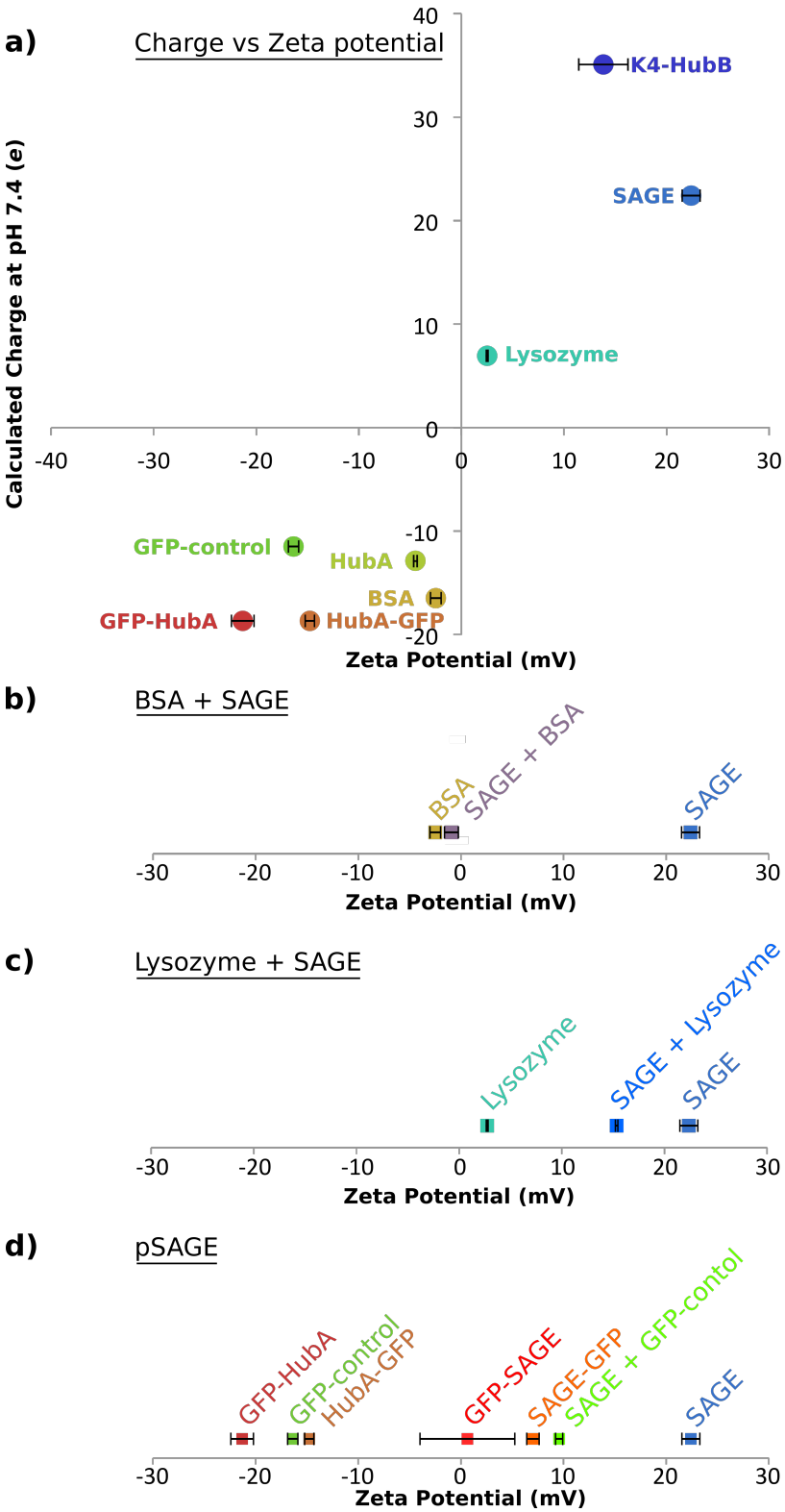

Figure S8: Calculated charge and measured zeta potential for pSAGE particles and their components. **(a)** A comparison of calculated charge (using the amino acid pKa values at pH 7.4) against the observed zeta potential for the components of the pSAGE particles. The final concentration of all solutions was 3 μM in peptide (ie 1.5 μM HubA with 1.5 μM K4-HubB for the SAGE preparations, 3 μM for just HubA preparation), except for the 'SAGE +' preparations, which contained 3 μM SAGE peptides plus 5% (0.15 μM) of the free protein. The change in zeta potential between protein, SAGE and pSAGE for **(a)** free BSA, **(b)** free HEWL and **(c)** free GFP-contol and incorporated GFP-SAGE and SAGE-GFP. These panels

show that there is greater association between SAGE and BSA than between SAGE and HEWL.

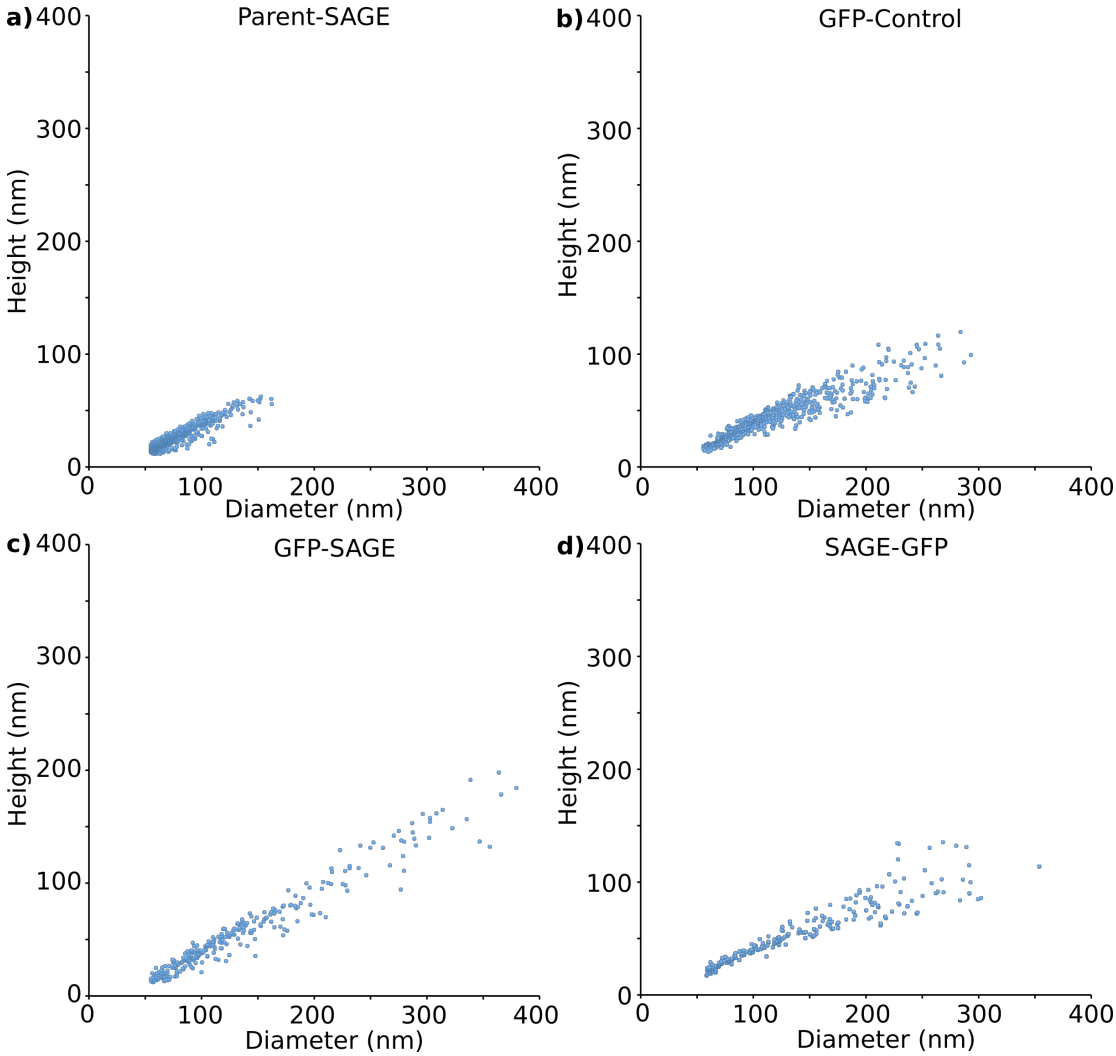

Figure S9: Single particle height and diameter AFM measurements of 25 μM SAGE and pSAGE constructs. **(a)** Parent-SAGE, **(b)** 5% GFP-control, **(c)** 5% GFP-SAGE and **(d)** 5% SAGE-GFP height vs diameter measurements on an individual particle basis.

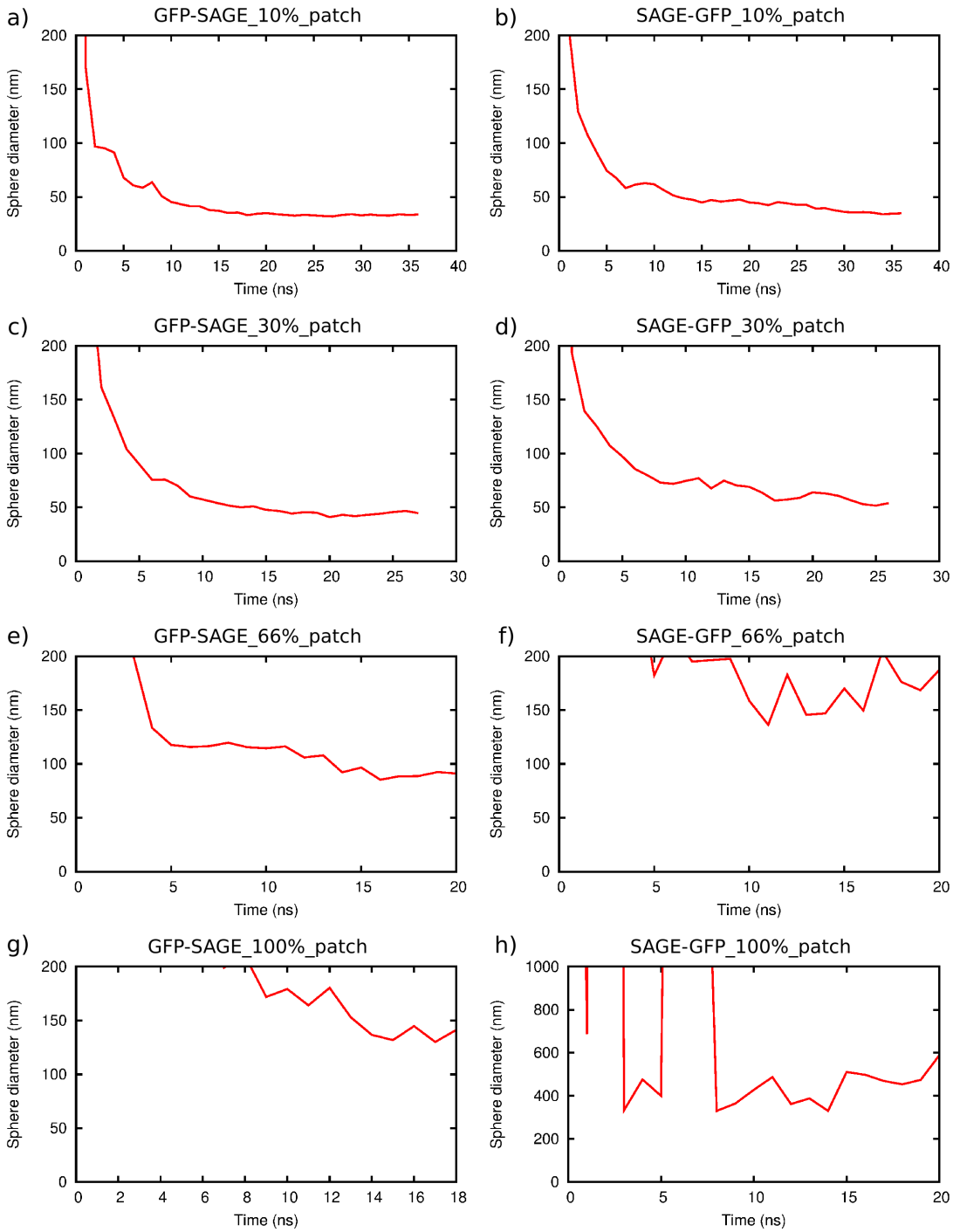

Figure S10: Estimations of the diameter of SAGE particles based on molecular dynamics. Molecular dynamics of 19 hexagon patches of SAGE assemblies were conducted with (**a, c, e and g**) GFP-SAGE and **(b, d, f and h)** SAGE-GFP with (**a and b)** 10% fusion protein, **(c and d)** 30% fusion protein, **(e and f)** 66% fusion protein and **(g and h)** 100% fusion protein. Diameters were estimated by fitting the positions of each SG atom (central and evenly spaced throughout the assembly) onto a sphere to find a best fitting diameter.

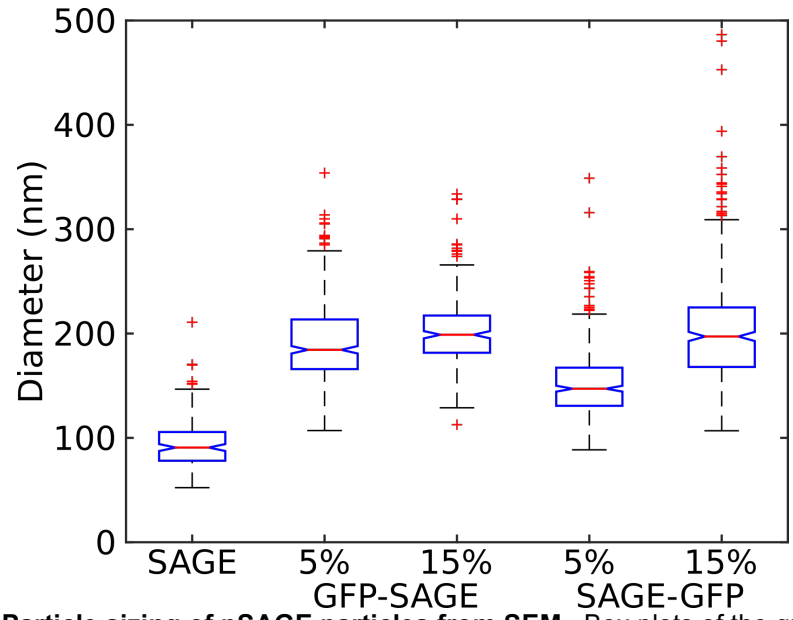

Figure S11: Particle sizing of pSAGE particles from SEM. Box plots of the grain sizing of SEM images for 25 μM parent-SAGE and both 5% and 15% GFP-SAGE and SAFE-GFP. The median is displayed in a red line, the interquartile range in the box, the whiskers are at the 5% and 95% confidence intervals and outliers are plotted as red pluses.

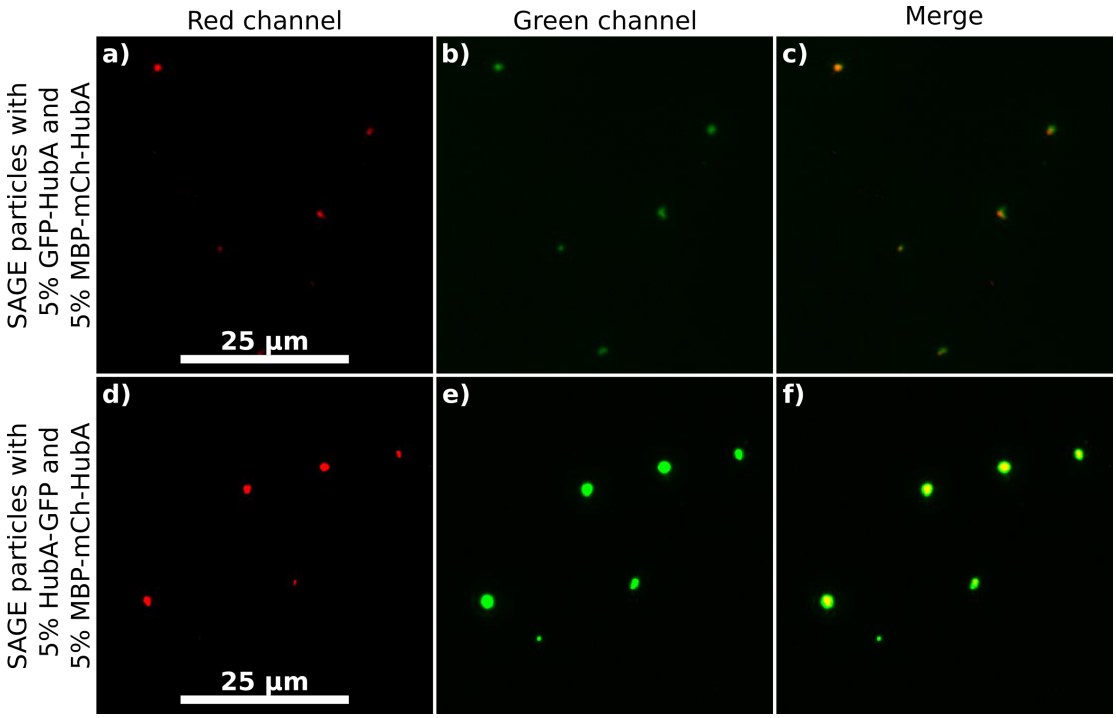

Figure S12: Correlation between GFP and mCherry fluorescence in SAGES. (a-c) The red, green and merged channel for 3 μM SAGE particels made containing 5% GFP-HubA and 5% MBP-mCh-SAGE. **(d-f)** The red, green and merged channel for 3μM SAGE particles made containing 5% HubA-GFP and 5% MBP-mCh-SAGE.

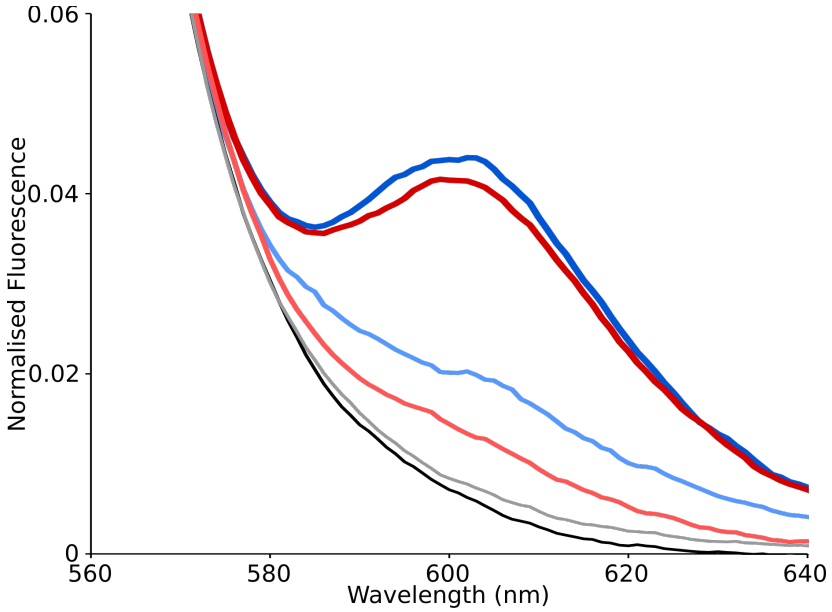

Figure S13: FRET signal between GFP and mCherry SAGE particles. All samples contain 1.5 μM HubA. Blue and red curves contain 5% MBP-mCh-HubA, blue curves contain 5% GFP-HubA, red curves contain 5% HubA-GFP. Dark blue and dark red curves contain 1.5 μM HubB and thus form SAGE particles, light blue and light red curves do not contain HubB and thus do not form SAGE particles. Black curve contains GFP-SAGE, Grey curve contains HubA-GFP.

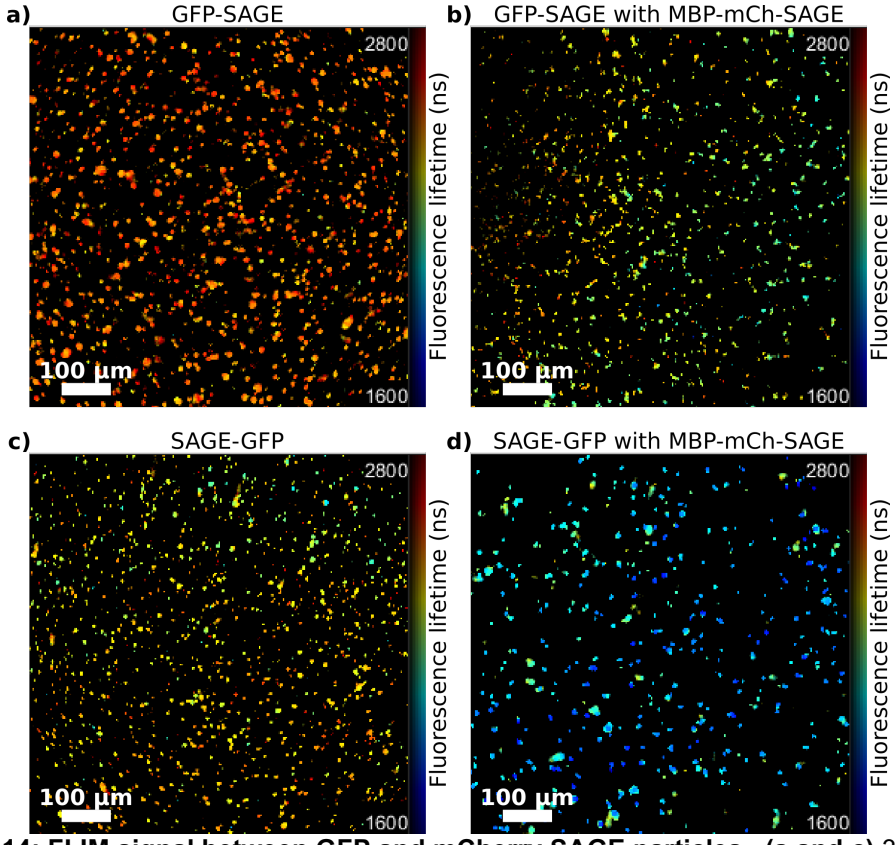

Figure S14: FLIM signal between GFP and mCherry SAGE particles. (a and c) 3 μM, 5% GFP-SAGE and SAGE-GFP, respectively. **(b and d)** As with a and d but allow including 5% MBP-mCh-HubA in the assembly. There is a loss in the fluorescene lifetime of the GFP when assembled into SAGE particles in the presence of MBP-mCh-HubA.

>GFP-control

MGTGGSGGGSGSTMSKGEELFTGVVPILVELDGDVNGHKFSVSGEGEGDATYGKLTLKFISTTGKLPVPWPT

LVTTLTYGVQMFARYPDHMKQHDFFKSAMPEGYVQERTIFFKDDGNYKTRAEVKFEGDTLVNRIELKGIDFK

EDGNILGHKLEYNYNSHNVYITADKQKNGIKANFKIRHNIEDGGVQLADHYQQNTPIGDGPVLLPDNHYLST

QSKLSKDPNEKRDHMVLLEFVTAAGITHGMDELYKASHHHHHH*

KEY : SEG-linker (tuncated) : cfGFP : HisTag

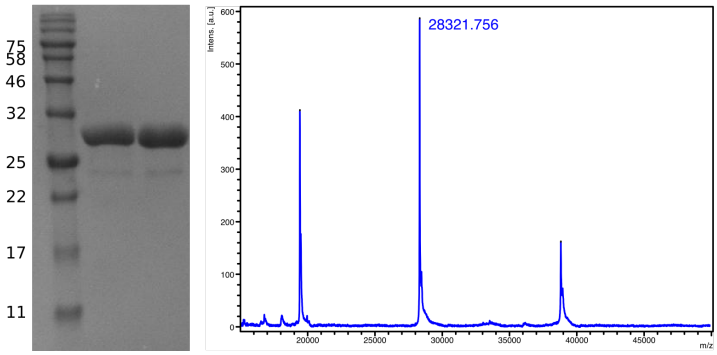

	Expected	Observed
GFP-control	28808	28321

Figure S15: Construct information and charaterisation for GFP-control. Schematic, anotated protein sequence, SDS-page and MALDI-TOF mass spectrometry of GFP-control.

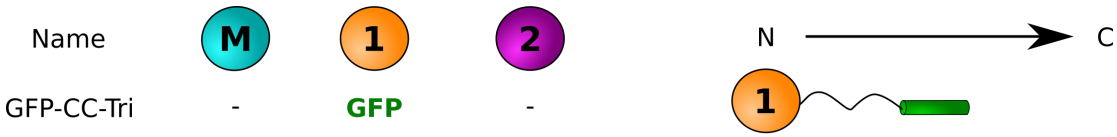

>GFP-CC-Tri

MGSAG**HHHHHH**GNS**MSKGEELFTGVVPILVELDGDVNGHKFSVSGEGEGDATYGKLTLKFISTTGKLPVPWP**

TLVTTLTYGVQMFARYPDHMKQHDFFKSAMPEGYVQERTIFFKDDGNYKTRAEVKFEGDTLVNRIELKGIDF

KEDGNILGHKLEYNYNSHNVYITADKQKNGIKANFKIRHNIEDGGVQLADHYQQNTPIGDGPVLLPDNHYLS

TQSKLSKDPNEKRDHMVLLEFVTAAGITHGMDELYKGT**GGSGGGSEGGGSEGGGSEGGGSEGGGSEGGGSGG**

GSGST**EIAAIKKEIAAIKCEIAAIKQ**AS**DYKDDDDK***

KEY : **HisTag** : **cfGFP** : **SEG-linker** : **CCtri** : **FlagTag**

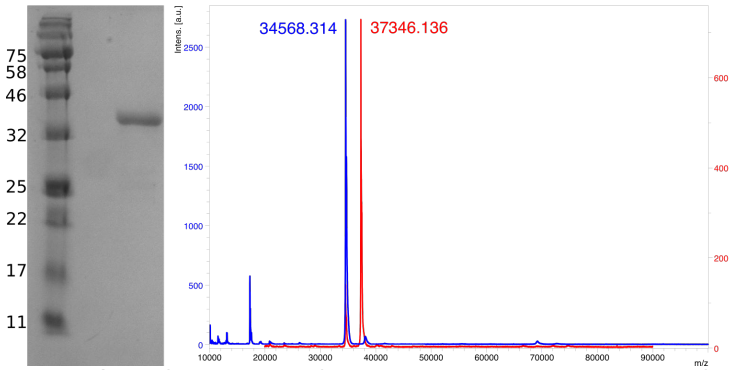

	Expected	Observed
GFP-CCTri	34763	34568
GFP-HubA	37548	37346
Modification	2784	2778

Figure S16: Construct information and charaterisation for GFP-CCtri. Schematic, anotated protein sequence, SDS-page. MALDI-TOF mass spectrometry of GFP-CCtri and GFP-HubA confirming modification by CC-DiA.

MGSAGDYKDDDDKGNSEIAAIKKEIAAIKCEIAAIKQGTGGSGGGSEGGGSEGGGSEGGGSEGGGSEGGGSG

GGSGSTMSKGEELFTGVVPILVELDGDVNGHKFSVSGEGEGDATYGKLTLKFISTTGKLPVPWPTLVTTLTY

GVQMFARYPDHMKQHDFFKSAMPEGYVQERTIFFKDDGNYKTRAEVKFEGDTLVNRIELKGIDFKEDGNILG

HKLEYNYNSHNVYITADKQKNGIKANFKIRHNIEDGGVQLADHYQQNTPIGDGPVLLPDNHYLSTQSKLSKD

PNEKRDHMVLLEFVTAAGITHGMDELYKASHHHHHH*

KEY : FlagTag : CCtri : SEG-linker : cfGFP : HisTag

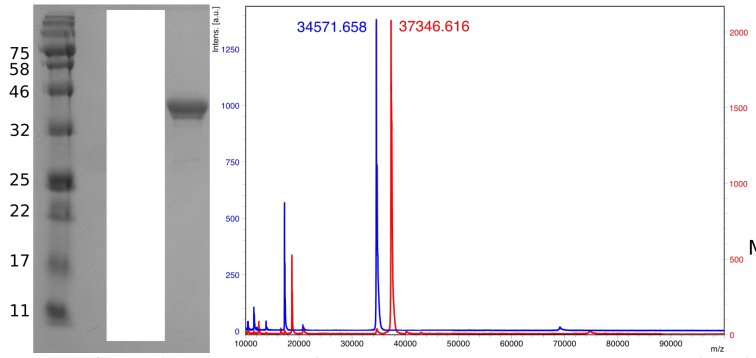

	Expected	Observed
GFP-CCTri	34763	34571
GFP-HubA	37548	37346
Modification	2784	2775

Figure S17: Construct information and charaterisation for CCtri-GFP. Schematic, anotated protein sequence, SDS-page. MALDI-TOF mass spectrometry of CCtri-GFP and HubA-GFP confirming modification by CC-DiA.

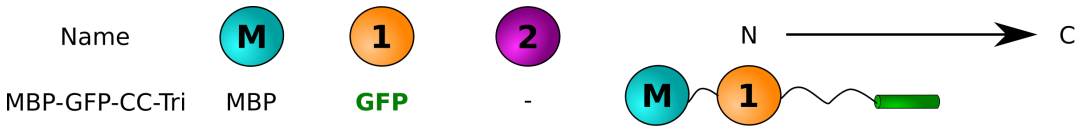

>MBP-GFP-CCtri

MGHHHHHHMGSGSGSGMKIEEGKLVIWINGDKGYNGLAEVGKKFEKDTGIKVTVEHPDKLEEKFPQVAATGDG

PDIIFWAHDRFGGYAQSGLLAEITPDKAFQDKLYPFTWDAVRYNGKLIAYPIAVEALSLIYNKDLLPNPPKTW

EEIPALDKELKAKGKSALMFNLQEPYFTWPLIAADGGYAFKYENGKYDIKDVGVDNAGAKAGLTFLVDLIKNK

HMNADTDYSIAEAAFNKGETAMTINGPWAWSNIDTSKVNYGVTVLPTFKGQPSKPFVGVLSAGINAASPNKEL

AKEFLENYLLTDEGLEAVNKDKPLGAVALKSYEEELAKDPRIAATMENAQKGEIMPNIPQMSAFWYAVRTAVI

NAASGRQTVDEALKDAQTGSGSENLYFQSSAGHHHHHHGNSMSKGEELFTGVVPILVELDGDVNGHKFSVSGE

GEGDATYGKLTLKFISTTGKLPVPWPTLVTTLTYGVQMFARYPDHMKQHDFFKSAMPEGYVQERTIFFKDDGN

YKTRAEVKFEGDTLVNRIELKGIDFKEDGNILGHKLEYNYNSHNVYITADKQKNGIKANFKIRHNIEDGGVQL

ADHYQQNTPIGDGPVLLPDNHYLSTQSKLSKDPNEKRDHMVLLEFVTAAGITHGMDELYKGTGGSGGGSEGGG

SEGGGSEGGGSEGGGSEGGGSGGGSGSTEIAAIKKEIAAIKCEIAAIKQASDYKDDDDK*

KEY : HisTag : MBP : TEV : HisTag : cfGFP : SEG-linker : CCtri : FlagTag

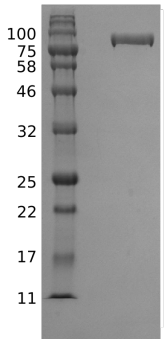

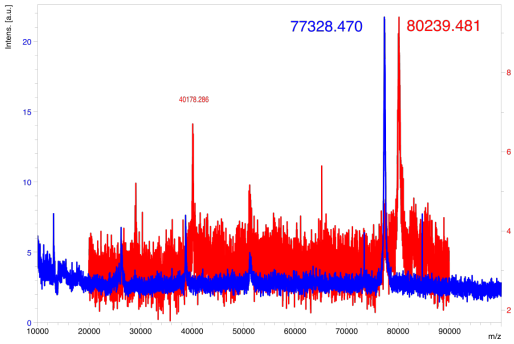

	Expected	Observed
MBP-GFP-CCTri	77699	77328
MBP-GFP-HubA	80483	80239
Modification	2784	2911

Figure S18: Construct information and charaterisation for MBP-GFP-CCtri. Schematic, anotated protein sequence, SDS-page. MALDI-TOF mass spectrometry of MBP-GFP-CCtri and MBP-GFP-HubA confirming modification by CC-DiA.

>MBP-CCTri-GFP

MGHHHHHHMGSGSGSGMKIEEGKLVIWINGDKGYNGLAEVGKKFEKDTGIKVTVEHPDKLEEKFPQVAATGD

GPDIIFWAHDRFGGYAQSGLLAEITPDKAFQDKLYPFTWDAVRYNGKLIAYPIAVEALSLIYNKDLLPNPPK

TWEEIPALDKELKAKGKSALMFNLQEPYFTWPLIAADGGYAFKYENGKYDIKDVGVDNAGAKAGLTFLVDLI

KNKHMNADTDYSIAEAAFNKGETAMTINGPWAWSNIDTSKVNYGVTVLPTFKGQPSKPFVGVLSAGINAASP

NKELAKEFLENYLLTDEGLEAVNKDKPLGAVALKSYEEELAKDPRIAATMENAQKGEIMPNIPQMSAFWYAV

RTAVINAASGRQTVDEALKDAQTGSGSENLYFQSSAGDYKDDDDKGNSEIAAIKKEIAAIKCEIAAIKQGTG

GSGGGSEGGGSEGGGSEGGGSEGGGSEGGGSGGGSGSTMSKGEELFTGVVPILVELDGDVNGHKFSVSGEGE

GDATYGKLTLKFISTTGKLPVPWPTLVTTLTYGVQMFARYPDHMKQHDFFKSAMPEGYVQERTIFFKDDGNY

KTRAEVKFEGDTLVNRIELKGIDFKEDGNILGHKLEYNYNSHNVYITADKQKNGIKANFKIRHNIEDGGVQL

ADHYQQNTPIGDGPVLLPDNHYLSTQSKLSKDPNEKRDHMVLLEFVTAAGITHGMDELYKASHHHHHH*

KEY : HisTag : MBP : TEV : FlagTag : CCtri : SEG-linker : cfGFP : HisTag

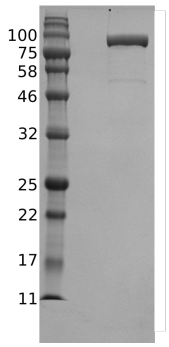

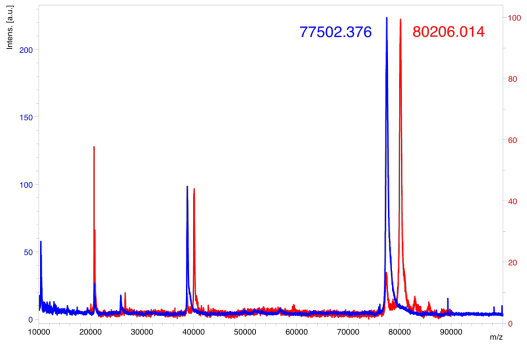

	Expected	Observed
MBP-CCtri-GFP	77699	77502
MBP-HubA-GFP	80483	80206
Modification	2784	2704

Figure S19: Construct information and charaterisation for MBP-CCtri-GFP. Schematic, anotated protein sequence, SDS-page. MALDI-TOF mass spectrometry of MBP-CCtri-GFP and MBP-HubA-GFP confirming modification by CC-DiA.

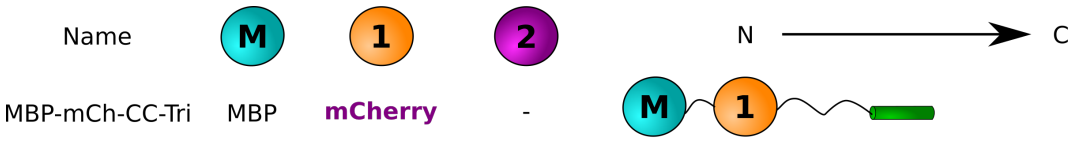

>MBP-mCh-CC-Tri

MGHHHHHHMGSGSGSGMKIEEGKLVIWINGDKGYNGLAEVGKKFEKDTGIKVTVEHPDKLEEKFPQVAATGD

GPDIIFWAHDRFGGYAQSGLLAEITPDKAFQDKLYPFTWDAVRYNGKLIAYPIAVEALSLIYNKDLLPNPPK

TWEEIPALDKELKAKGKSALMFNLQEPYFTWPLIAADGGYAFKYENGKYDIKDVGVDNAGAKAGLTFLVDLI

KNKHMNADTDYSIAEAAFNKGETAMTINGPWAWSNIDTSKVNYGVTVLPTFKGQPSKPFVGVLSAGINAASP

NKELAKEFLENYLLTDEGLEAVNKDKPLGAVALKSYEEELAKDPRIAATMENAQKGEIMPNIPQMSAFWYAV

RTAVINAASGRQTVDEALKDAQTGSGSENLYFQSSAGHHHHHHGNSMVSKGEEDNMAIIKEFMRFKVHMEGS

VNGHEFEIEGEGEGRPYEGTQTAKLKVTKGGPLPFAWDILSPQFMYGSKAYVKHPADIPDYLKLSFPEGFKW

ERVMNFEDGGVVTVTQDSSLQDGEFIYKVKLRGTNFPSDGPVMQKKTMGWEASSERMYPEDGALKGEIKQRL

KLKDGGHYDAEVKTTYKAKKPVQLPGAYNVNIKLDITSHNEDYTIVEQYERAEGRHSTGGMDELYKGTGGSG

GGSEGGGSEGGGSEGGGSEGGGSEGGGSGGGSGSTEIAAIKKEIAAIKCEIAAIKQASDYKDDDDK*

KEY : SEG-linker : cfGFP : HisTag

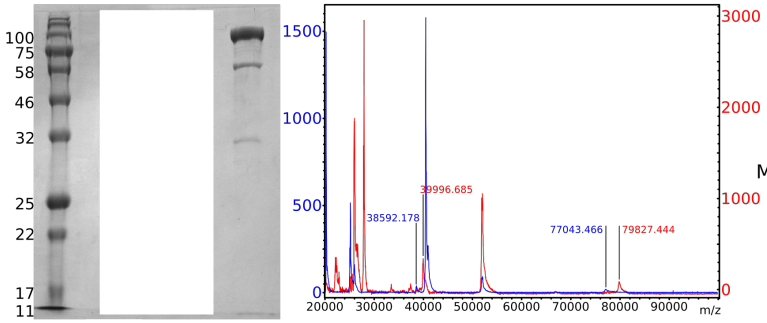

	Expected	Observed
MBP-mCh-CCTri	77589	77043
MBP-mCh--HubA	80374	79827
Modification	2784	2784

Figure S20: Construct information and charaterisation for MBP-mCh-CCtri. Schematic, anotated protein sequence, SDS-page (showing minor degredation products). MALDI-TOF mass spectrometry of MBP-mch-CCtri and MBP-mCh-HubA confirming modification by CC-DiA (the full length product was not readily detectable by mass spectrometry, hence only a small peak was obtained).

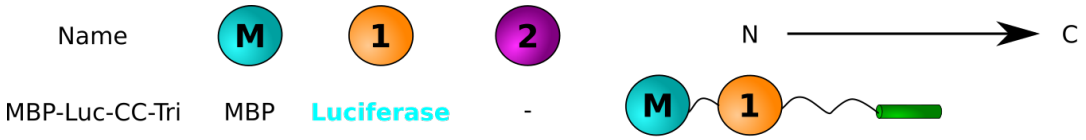

>MBP-Luc-CC-Tri

MGHHHHHHMGSGSGSGMKIEEGKLVIWINGDKGYNGLAEVGKKFEKDTGIKVTVEHPDKLEEKFPQVAATGD

GPDIIFWAHDRFGGYAQSGLLAEITPDKAFQDKLYPFTWDAVRYNGKLIAYPIAVEALSLIYNKDLLPNPPK

TWEEIPALDKELKAKGKSALMFNLQEPYFTWPLIAADGGYAFKYENGKYDIKDVGVDNAGAKAGLTFLVDLI

KNKHMNADTDYSIAEAAFNKGETAMTINGPWAWSNIDTSKVNYGVTVLPTFKGQPSKPFVGVLSAGINAASP

NKELAKEFLENYLLTDEGLEAVNKDKPLGAVALKSYEEELAKDPRIAATMENAQKGEIMPNIPQMSAFWYAV

RTAVINAASGRQTVDEALKDAQTGSGSENLYFQSSAGHHHHHHGNSMTSKVYDPEQRKRMITGPQWWARCKQ

MNVLDSFINYYDSEKHAENAVIFLHGNAASSYLWRHVVPHIEPVARCIIPDLIGMGKSGKSGNGSYRLLDHY

KYLTAWFELLNLPKKIIFVGHDWGACLAFHYSYEHQDKIKAIVHAESVVDVIESWDEWPDIEEDIALIKSEE

GEKMVLENNFFVETMLPSKIMRKLEPEEFAAYLEPFKEKGEVRRPTLSWPREIPLVKGGKPDVVQIVRNYNA

YLRASDDLPKMFIESDPGFFSNAIVEGAKKFPNTEFVKVKGLHFSQEDAPDEMGKYIKSFVERVLKNEQGTG

GSGGGSEGGGSEGGGSEGGGSEGGGSEGGGSGGGSGSTEIAAIKKEIAAIKCEIAAIKQASDYKDDDDK*

KEY : HisTag : MBP : TEV : HisTag : Luc : SEG-linker : CCtri : FlagTag

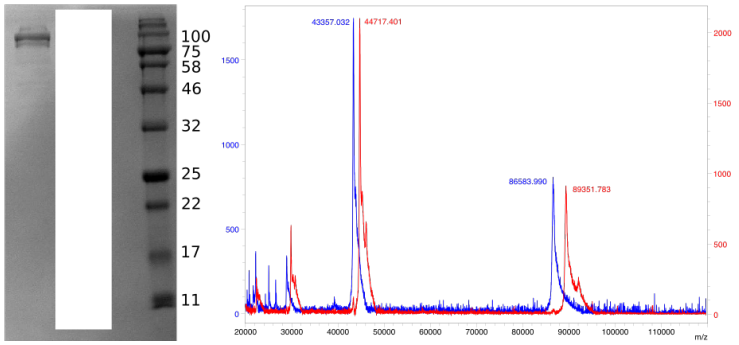

	Expected	Observed
MBP-Luc-CCTri	86890	86583
MBP-Luc-HubA	89674	89351
Modification	2784	2768

Figure S21: Construct information and charaterisation for MBP-Luc-CCtri. Schematic, anotated protein sequence, SDS-page. MALDI-TOF mass spectrometry of MBP-Luc-CCtri and MBP-Luc-HubA confirming modification by CC-DiA.

>MBP-CC-Tri-Luc

MGHHHHHHMGSGSGSGMKIEEGKLVIWINGDKGYNGLAEVGKKFEKDTGIKVTVEHPDKLEEKFPQVAATGD

GPDIIFWAHDRFGGYAQSGLLAEITPDKAFQDKLYPFTWDAVRYNGKLIAYPIAVEALSLIYNKDLLPNPPK

TWEEIPALDKELKAKGKSALMFNLQEPYFTWPLIAADGGYAFKYENGKYDIKDVGVDNAGAKAGLTFLVDLI

KNKHMNADTDYSIAEAAFNKGETAMTINGPWAWSNIDTSKVNYGVTVLPTFKGQPSKPFVGVLSAGINAASP

NKELAKEFLENYLLTDEGLEAVNKDKPLGAVALKSYEEELAKDPRIAATMENAQKGEIMPNIPQMSAFWYAV

RTAVINAASGRQTVDEALKDAQTGSGSENLYFQSSAGDYKDDDDKGNSEIAAIKKEIAAIKCEIAAIKQGTG

GSGGGSEGGGSEGGGSEGGGSEGGGSEGGGSGGGSGSTMTSKVYDPEQRKRMITGPQWWARCKQMNVLDSFI

NYYDSEKHAENAVIFLHGNAASSYLWRHVVPHIEPVARCIIPDLIGMGKSGKSGNGSYRLLDHYKYLTAWFE

LLNLPKKIIFVGHDWGACLAFHYSYEHQDKIKAIVHAESVVDVIESWDEWPDIEEDIALIKSEEGEKMVLEN

NFFVETMLPSKIMRKLEPEEFAAYLEPFKEKGEVRRPTLSWPREIPLVKGGKPDVVQIVRNYNAYLRASDDL

PKMFIESDPGFFSNAIVEGAKKFPNTEFVKVKGLHFSQEDAPDEMGKYIKSFVERVLKNEQASHHHHHH*

KEY : HisTag : MBP : TEV : FlagTag : CCtri : SEG-linker : Luc : HisTag

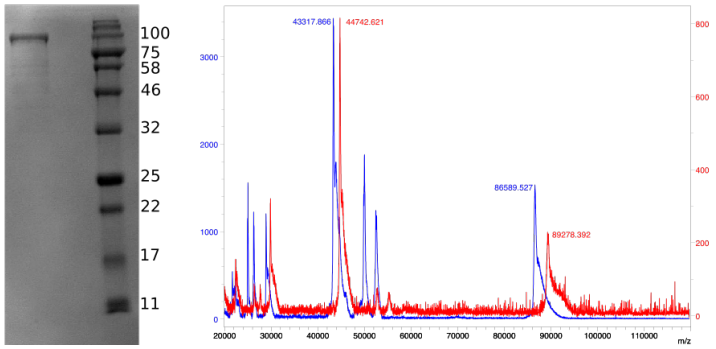

	Expected	Observed
MBP-CCtri-Luc	86890	86589
MBP-HubA-Luc	89674	89278
Modification	2784	2689

Figure S22: Construct information and charaterisation for MBP-CCtri-Luc. Schematic, anotated protein sequence, SDS-page. MALDI-TOF mass spectrometry of MBP-CCtri-Luc and MBP-HubA-Luc confirming modification by CC-DiA.